

Leptonic neutral-current probes in a short-distance DUNE-like setup

Salvador Centelles Chuliá,^{1,*} O. G. Miranda,^{2,†} and Jose W.F. Valle^{3,‡}

¹*Max-Planck-Institut für Kernphysik, Saupfercheckweg 1, 69117 Heidelberg, Germany*

²*Departamento de Física, Centro de Investigación y de Estudios Avanzados del IPN Apdo. Postal 14-740 07000 Ciudad de México, México*

³*AHEP Group, Institut de Física Corpuscular – CSIC/Universitat de València, Parc Científic de Paterna. C/ Catedrático José Beltrán, 2 E-46980 Paterna (Valencia), Spain*

Precision measurements of neutrino-electron scattering may provide a viable way to test the non-minimal form of the charged and neutral current weak interactions within a hypothetical near-detector setup for the Deep Underground Neutrino Experiment (DUNE). Although low-statistics, these processes are clean and provide information complementing the results derived from oscillation studies. They could shed light on the scale of neutrino mass generation in low-scale seesaw schemes.

I. INTRODUCTION

Ever since the historic discovery of neutrino oscillations [1, 2] indicating the need for neutrino masses, most progress in neutrino physics has relied on experiments involving charged current (CC) processes. However, the observation of coherent elastic neutrino-nucleus scattering (CEvNS) [3, 4] proposed long ago in the pioneer papers [5, 6], has prompted a neutral current (NC) *revival* and the recognition that the NC can provide an interesting and complementary way to study neutrinos.

Moreover, it has long been known from theory that, if neutrino mass generation is mediated by heavy neutrino exchange, the structure of both the CC and NC is non-trivial [7, 8]. Indeed, the mixing matrix K characterizing the leptonic CC weak interaction that describes oscillations is not unitary, while the NC interaction of mass-eigenstate neutrinos involves a matrix P that deviates from the unit matrix. Moreover, these two matrices are related [7, 8].

Although the effect of non-unitary neutrino mixing was first discussed in the context of astrophysical neutrino propagation [9–11], it can be phenomenologically relevant in earth-bound experiments. This happens in the context of genuine low-scale seesaw schemes, such as the inverse [12, 13] or the linear seesaw mechanism [14–16], leading to potentially sizeable deviations from the conventional leptonic weak currents with unitary CC mixing. These corrections are expressed as power series in the parameter $\varepsilon = \mathcal{O}(Yv/M)$, where M is the mediator mass scale and v is the SM vacuum expectation value (vev). Although small, we stress that ε can be non-negligible within low-scale realisations of the seesaw. The effects of unitarity violation and the new associated neutrino phenomena have been extensively explored in the recent literature, mainly devoted to charged-current processes

* chulia@mpi-hd.mpg.de

† omar.miranda@investav.mx

‡ valle@ific.uv.es

on hadronic probes [17–42].

Here we explore the potential of leptonic probes such as the scattering process $\nu + e^- \rightarrow \nu + e^-$ as a potentially viable way to test the non-minimal form of the CC and NC weak interactions. This has already been discussed in [43, 44] in the context of hadronic probes. In this paper we speculate that leptonic probes, too, may be useful within a DUNE-like near-detector setup. Although low-statistics, these processes are clean and provide information complementing the results derived from oscillation studies [45], shedding light on the scale of neutrino mass generation within low-scale seesaw schemes.

II. THEORY PRELIMINARIES

The most general CC weak interaction of massive neutrinos is described by a rectangular matrix K [7]. A short summary of the main features and notation is as follows. In the basis where the charged lepton mass matrix is diagonal, the upper blocks are simply the first 3 rows of the neutrino mixing matrix [8]. We can also define the relevant sub-block as

$$K = \begin{pmatrix} N & S \end{pmatrix} \quad (1)$$

With 3 active neutrino flavours, N is a 3×3 matrix, while S is a $3 \times m$ matrix, with m the number of fermionic singlets that mix with the active neutrinos¹. The small block $S \sim \mathcal{O}(\varepsilon)$ is the seesaw expansion matrix [8]. Notice that $KK^\dagger = I_{3 \times 3}$ and therefore $NN^\dagger = 1 - SS^\dagger \sim 1 - \mathcal{O}(\varepsilon^2)$. On the other hand, the matrix P describing the NC-neutrino interactions [7] is given by

$$P = K^\dagger K \neq I. \quad (2)$$

If the energy of a given process is much lower than the masses of the heavy mediators these will not be produced. For example, the heavy states will not take part in oscillation experiments. Then, effectively, only the first 3×3 blocks of K and P will play a role in the weak interactions, i.e. N in the charged current and $N^\dagger N$ in the neutral current. This would signal the presence of unitarity violation in the neutrino mixing matrix [9] whose general description is given in [17]. A systematic approach to the (non-unitary) matrix N can be derived from the seesaw expansion [8], as the lower triangular parametrization proposed in [17]².

$$N = \begin{pmatrix} \alpha_{11} & 0 & 0 \\ \alpha_{21} & \alpha_{22} & 0 \\ \alpha_{31} & \alpha_{31} & \alpha_{33} \end{pmatrix} \cdot U \quad (3)$$

Besides the 3×3 unitary matrix U used to describe neutrino mixing in the conventional unitary case, one has the triangular pre-factor characterized by 3 diagonal α_{ii} ($i = 1, 2, 3$), real and close to 1, and 3 non-diagonal α_{ij} ($i \neq j$) which are small but complex. This is a convenient and complete description of non-unitarity. By

¹ In the most general SM-seesaw one can have any number of “right-handed” neutrino mediators, since they are gauge singlets [7].

² An alternative description and its relationship with Eq. 3 is discussed in Ref. [46]

construction, N and S must satisfy the relation $NN^\dagger = 1 - SS^\dagger$, hence $NN^\dagger \sim 1 - \mathcal{O}(\varepsilon^2)$. Explicitly,

$$NN^\dagger = \begin{pmatrix} \alpha_{11}^2 & \alpha_{11}\alpha_{21}^* & \alpha_{11}\alpha_{31}^* \\ \alpha_{11}\alpha_{21} & \alpha_{22}^2 + |\alpha_{21}|^2 & \alpha_{22}\alpha_{32}^* + \alpha_{21}\alpha_{31}^* \\ \alpha_{11}\alpha_{31} & \alpha_{22}\alpha_{32} + \alpha_{21}^*\alpha_{31} & \alpha_{33}^2 + |\alpha_{31}|^2 + |\alpha_{32}|^2 \end{pmatrix}, \quad (4)$$

from where one can read off the strength of the α_{ij} in terms of the small seesaw expansion parameter ε . Indeed, within the seesaw paradigm, the leading deviation from the standard form of the CC mixing matrix lies in the diagonal entries $NN^\dagger \sim 1 - \mathcal{O}(\varepsilon^2)$ implying that, for example, $\alpha_{11}^2 \sim 1 - \mathcal{O}(\varepsilon^2)$. Hence $\alpha_{11}\alpha_{21} \sim \mathcal{O}(\varepsilon^2)$, so that $\alpha_{21} \sim \mathcal{O}(\varepsilon^2)$ and

$$\alpha_{ii}^2 \sim 1 - \mathcal{O}(\varepsilon^2) \quad (5)$$

$$|\alpha_{ij}|^2 \sim \mathcal{O}(\varepsilon^4), \quad i \neq j. \quad (6)$$

One sees that the the strength of the off-diagonal α 's is suppressed relative to the deviations of the flavor-diagonal ones from their SM values. In other words, in the seesaw expansion the 0th order corresponds to the unitary limit, the 1st order gives only diagonal flavour-conserving effects, while the genuine flavour-violating effects non-unitary corrections only come at 2nd order. Notice also that this behavior is consistent with the validity of the well-known triangle inequality $|\alpha_{ij}| \leq \sqrt{(1 - \alpha_{ii}^2)(1 - \alpha_{jj}^2)}$ [17].

Additionally, it is important to notice that unitarity violation leads to a redefinition of the Fermi constant, extracted from the μ^- lifetime assuming the SM. In the presence of non-unitarity the measured quantity would be the effective muon decay coupling G_μ . Since the W-boson vertices are modified by the non-unitarity parameters one finds

$$G_\mu = 1.1663787(6) \times 10^{-5} \text{ GeV}^{-2} \quad (\text{effective } \mu^- \text{ decay constant, [47]}) \quad (7)$$

$$G_\mu^2 = G_F^2 (NN^\dagger)_{ee} (NN^\dagger)_{\mu\mu} \quad (8)$$

And therefore

$$1 \leq \frac{G_F^2}{G_\mu^2} = \frac{1}{(NN^\dagger)_{ee}(NN^\dagger)_{\mu\mu}} \approx 3 - \alpha_{11}^2 - \alpha_{22}^2 \sim 1 + \mathcal{O}(\varepsilon^2) \quad (9)$$

Therefore, in the presence of non-unitarity any process proportional to G_F^2 will get an ‘‘enhancement’’. This is counter-intuitive, because naively one expects less events than in the SM if the mixing is non-unitary, due to kinematically inaccessible heavy states. The reduction of the event number due to non-unitarity and the ‘‘increase’’ due to the redefinition of G_F compete with each other, so that in some cases one can achieve $\mathcal{N}_{\text{NU}}/\mathcal{N}_{\text{U}} = 1$ even in the presence of non-unitarity.

III. $\nu_\mu - e^-$ SCATTERING IN THE PRESENCE OF NON-UNITARITY AT ZERO DISTANCE

We now turn our attention to the scattering of a muon neutrino on an electron target in the presence of non-unitarity. The relevant Feynman diagrams, given in Figs. 1 and 2, describe the elastic electron-neutrino scattering and the neutrino-induced muon production processes, respectively.

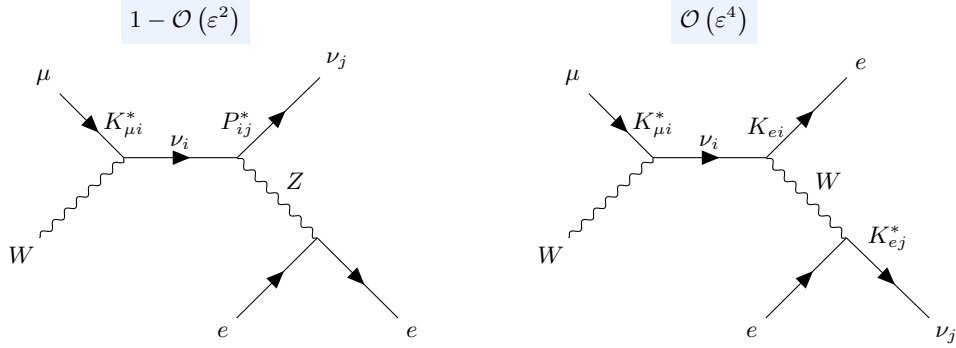


FIG. 1. Feynman diagrams for $\nu_\mu + e^-$ scattering, where the ν_μ is produced via the usual CC vertex, while the final-state detection involves the NC (left diagram), with a sub-leading CC contribution, of order ε^4 (right diagram).

A. Neutrino-electron elastic scattering

At tree level the two relevant diagrams are given in Fig. 1. The vertex on the left of each diagram corresponds to CC ν_μ production, while the vertex on the right depicts either the NC and CC detection modes, respectively. Within the three neutrino paradigm, with unitary lepton mixing, the CC channel (right panel of Fig. 1) does not contribute at zero distance. In such case, the process is pure NC (left panel of Fig. 1) and the differential cross-section is given by

$$\left(\frac{d\sigma}{dT}\right)^{\text{SM}} = \frac{2G_\mu^2 m_e}{\pi} \left(g_L^2 + g_R^2 \left(1 - \frac{T}{E\nu}\right)^2 - g_L g_R \frac{m_e T}{E_\nu^2} \right) \quad (10)$$

where $g_L = -1/2 + \sin^2 \theta_W$ and $g_R = -\sin^2 \theta_W$. However, in the presence of non-unitarity the CC contribution is in general non-zero. In this case, the cross section is replaced by

$$\left(\frac{d\sigma}{dT}\right)^{\text{NU}} = \frac{\mathcal{P}_{\mu e}^{\text{NC}}}{(NN^\dagger)_{ee}(NN^\dagger)_{\mu\mu}} \left(\frac{d\sigma}{dT}\right)^{\text{SM}} + \frac{2m_e G_\mu^2}{\pi} \frac{\mathcal{R}e[\mathcal{P}_{\mu e}^{\text{int}}]}{(NN^\dagger)_{ee}(NN^\dagger)_{\mu\mu}} \left\{ \frac{\mathcal{P}_{\mu e}^{\text{CC}}}{\mathcal{R}e[\mathcal{P}_{\mu e}^{\text{int}}]} + 2g_L - g_R \frac{m_e T}{E_\nu^2} \right\}, \quad (11)$$

where the probability factors are given by

$$\mathcal{P}_{\mu e}^{\text{NC}} = (NN^\dagger NN^\dagger NN^\dagger)_{\mu\mu} \quad (12)$$

$$\mathcal{P}_{\mu e}^{\text{CC}} = (NN^\dagger)_{\mu e} (NN^\dagger)_{e\mu} (NN^\dagger)_{ee} \quad (13)$$

$$\mathcal{P}_{\mu e}^{\text{int}} = (NN^\dagger NN^\dagger)_{e\mu} (NN^\dagger)_{\mu e}. \quad (14)$$

Note that, in general, the slope of the differential cross-section in the presence of non-unitarity differs from that expected in the SM, as it changes the relative weight between the T -dependent and constant terms. This is determined by the actual values of the probability factors, in turn specified by the non-unitarity parameters α_{ij} . While the exact expression in Eq. 11 is a complicated function of the α_{ij} , one can write it in powers of the seesaw expansion parameter ε by following the prescription given in Eqs. 5 and 6. This implies that, to $\mathcal{O}(\varepsilon^2)$, the SM kinematic structure is preserved, and one has just an overall re-scaling compared to the SM expectation

$$\left(\frac{d\sigma}{dT}\right)^{\text{NU}} \approx (2\alpha_{22}^2 - \alpha_{11}^2) \left(\frac{d\sigma}{dT}\right)^{\text{SM}} + \mathcal{O}(\varepsilon^4). \quad (15)$$

This can be understood by expanding the NC probability factor in powers of ε and noticing that the leading term is of order $1 - \mathcal{O}(\varepsilon^2)$ and can be written as

$$\mathcal{P}_{\mu e}^{\text{NC}} = (NN^\dagger NN^\dagger NN^\dagger)_{\mu\mu} \approx 3\alpha_{22}^2 - 2 \sim 1 - \mathcal{O}(\varepsilon^2) , \quad (16)$$

while the CC and interference probability factors are instead $\mathcal{O}(\varepsilon^4)$, i.e.

$$\mathcal{P}_{\mu e}^{\text{CC}} = (NN^\dagger)_{\mu e} (NN^\dagger)_{e\mu} (NN^\dagger)_{ee} = \alpha_{11}^4 |\alpha_{21}|^2 \sim \mathcal{O}(\varepsilon^4) \quad (17)$$

$$\mathcal{P}_{\mu e}^{\text{int}} = (NN^\dagger NN^\dagger)_{e\mu} (NN^\dagger)_{\mu e} \approx 2|\alpha_{21}|^2 \sim \mathcal{O}(\varepsilon^4) , \quad (18)$$

Therefore, up to $\mathcal{O}(\varepsilon^2)$ terms one can neglect the CC and interference contributions, hence recovering the same kinematic structure characteristic of the SM and given by Eq. 10. Deviations from the SM kinematic structure come only at order $\mathcal{O}(\varepsilon^4)$, due to the interplay of both diagrams in Fig. 1, involving genuine flavour violating NU parameters $\alpha_{ij}, i \neq j$.

All in all, the ratio between the expected number of events in the unitary (\mathcal{N}_U) and the non-unitary (\mathcal{N}_{NU}) cases is given by

$$\frac{\mathcal{N}_{\text{NU}}}{\mathcal{N}_U} = \mathcal{P}_{\mu e}^{\text{NC}} \frac{G_F^2}{G_\mu^2} + \mathcal{O}(\varepsilon^4) = \frac{(NN^\dagger NN^\dagger NN^\dagger)_{\mu\mu}}{(NN^\dagger)_{ee} (NN^\dagger)_{\mu\mu}} \approx 2\alpha_{22}^2 - \alpha_{11}^2 . \quad (19)$$

Notice that, contrary to naive expectations, Eq. 19 can be either bigger or smaller than 1, due to the effect of the redefinition of G_F . Ideally, though, with very high statistics, one would be sensitive to the T -dependence change in the differential cross-section at $\mathcal{O}(\varepsilon^4)$ of Eq. 11.

B. Neutrino-induced muon production

For sufficiently energetic ($E_\nu > 10$ GeV) incoming neutrinos, an additional process with a muon in the final state becomes kinematically possible.

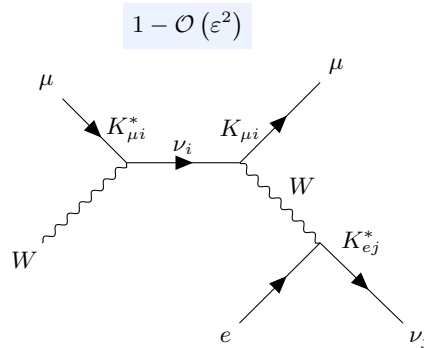


FIG. 2. Feynman diagram for the charged current process $\nu_\mu + e^- \rightarrow \nu + \mu^-$ in the non-unitary case.

As shown in Fig. 2, there is only one (CC) diagram contributing to this process. Therefore, its kinematical

structure is not modified at any order in the seesaw expansion,

$$\sigma^{(\text{SM})} \approx \frac{G_F^2}{\pi} (2E_\nu m_e - m_\mu^2), \quad (20)$$

so that the effect of non-unitarity translates only into an overall probability factor

$$\mathcal{P}_{\mu\mu} = (NN^\dagger)_{\mu\mu}^2 (NN^\dagger)_{e\epsilon} \approx 2\alpha_{22}^2 + \alpha_{11}^2 - 2 \sim 1 - \mathcal{O}(\varepsilon^2) \quad (21)$$

Taking into account also the redefinition of G_F we get

$$\frac{\mathcal{N}_{\text{NU}}}{\mathcal{N}_{\text{U}}} = \mathcal{P}_{\mu\mu} \frac{G_F^2}{G_\mu^2} = (NN^\dagger)_{\mu\mu} \approx \alpha_{22}^2 \leq 1 \quad (22)$$

In summary, leptonic probes such as electron-neutrino elastic scattering and neutrino-induced muon production have a rich phenomenology and a theoretically interesting structure that allows us to probe non-unitarity effects in a unique manner, as shown in Eqs. 11, 19 and 22.

IV. TESTING NON-UNITARITY IN THE NEUTRAL CURRENT AT A NEAR DETECTOR

Long-Baseline neutrino experiments require a near detector for a reliable flux calibration. They may give the opportunity to measure neutrino-electron scattering with good statistics. For example, DUNE is a planned particle physics experiment aimed at conducting in-depth studies of neutrinos. Scheduled to be hosted by Fermilab in the United States, the project's design includes sending a high-intensity neutrino beam over a distance of approximately 1,300 km from Fermilab in Illinois to a massive liquid-argon time-projection chamber in South Dakota. This far detector will be situated 1.5 km underground at the Sanford Underground Research Facility and is expected to have a total mass of around 40,000 metric tons. DUNE's main goals include investigating neutrino oscillations, exploring CP violation in the leptonic sector, and conducting astrophysical neutrino studies.

Several near detectors are under consideration for DUNE. We will focus our analysis on a detector with similar characteristics as that of the Liquid Argon Near-Detector (ND-LAr) located at a distance from the source similar to the one considered at DUNE. In general, near detectors are thought to measure the neutrino beam with high precision. This is essential for reducing systematic uncertainties in the data to be collected by any LBL far detector.

The two detectors will work in tandem, with the near-far configuration enabling more accurate and reliable data interpretation. By providing initial measurements and helping calibrate the far detector's data, DUNE near detectors will be integral to achieving the scientific aims of the DUNE experiment.

The neutrino beam at Fermilab, serving as the neutrino source, can operate in two distinct modes: neutrino and antineutrino. In each mode, the generated beam contains a contribution of four neutrino types: electron neutrinos, electron antineutrinos, muon neutrinos and muon antineutrinos. Depending on the operation mode, the main contribution is either muon neutrinos or muon antineutrinos in the beam. The main component of the flux, the muon (anti)neutrino, peaks at around 3 GeV, but also contains a long tail extending from 10 GeV to approximately 50 GeV.

In this article, we will delve into a near detector sensitivity to non-unitarity parameters through leptonic processes, taking into account specific design features mentioned above. In order to do so we will analyze the number of events in two distinct processes that can be measured separately: neutrino-electron elastic scattering and neutrino-induced muon production. Notice that the flavour composition of the incoming neutrino is given by the standard flux calculation, while the outgoing neutrinos cannot be distinguished individually and thus we sum over all the kinematically accessible mass states.

A. Elastic neutrino-electron scattering

Although the (anti)muon flavour dominates the flux in the (anti)neutrino mode, there are non-zero components of the 4 flavours/antiflavours involving e and μ . For each process, the number of events in the presence of lepton non-unitarity is calculated as

$$N_a^e = \mathcal{P}_a \mathcal{E} \int_{T_{\min}}^{T_{\max}(E_\nu)} \int_{E_\nu^{\min}(T')}^{\infty} \frac{d\sigma_a}{dT'}(E'_\nu, T') \lambda_a(E_\nu) dE'_\nu dT', \quad (23)$$

where the index a runs over $\{e, \bar{e}, \mu, \bar{\mu}\}$ and T is the detected electron kinetic energy, with the energy threshold in the detector being $T_{\min} = 0.2$ GeV. Here $\lambda_a(E_\nu)$ is the neutrino flux, while \mathcal{P}_a denotes the probability factor of that particular flavour. After neglecting the electron mass compared to T and E_ν we obtain $E_\nu^{\min}(T) = \frac{1}{2}(T_{\min} + \sqrt{T_{\min}^2 + 2T_{\min}m_e}) \approx T_{\min} = 0.2$ GeV and $T_{\max}(E_\nu) = \frac{2E_\nu^2}{2E_\nu + m_e} \approx E_\nu$. Finally, \mathcal{E} is the exposure, calculated as the product of the number of protons on target per year 1.1×10^{21} POT/year, the number of target electrons $N_t = 2 \times 10^{31}$ and the time spent in each mode $t = 3.5$ years. The resulting numbers are given in Tab. I. We present the expected number of events coming from each neutrino species within the unitary case as well as in the presence of non-unitarity. The probability factor includes the direct effect of the non-unitary lepton mixing matrix as well as the redefinition of G_F , expanded to the first order in the seesaw expansion parameter ε .

\mathcal{N}_U $\nu_a + e^- \rightarrow \nu_j + e^-$	ν mode		$\bar{\nu}$ mode		$\mathcal{N}_{NU}/\mathcal{N}_U$ $\mathcal{P} G_F^2/G_\mu^2$	Seesaw order	Main contribution
	events	σ	events	σ			
ν_e	2.800	80	1.530	50	$2\alpha_{11}^2 - \alpha_{22}^2$	$1 \pm \mathcal{O}(\varepsilon^2)$	NC + CC
ν_μ	31.400	700	5.800	100	$2\alpha_{22}^2 - \alpha_{11}^2$	$1 \pm \mathcal{O}(\varepsilon^2)$	NC
$\bar{\nu}_e$	430	20	780	30	$2\alpha_{11}^2 - \alpha_{22}^2$	$1 \pm \mathcal{O}(\varepsilon^2)$	NC + CC
$\bar{\nu}_\mu$	3.200	80	20.000	400	$2\alpha_{22}^2 - \alpha_{11}^2$	$1 \pm \mathcal{O}(\varepsilon^2)$	NC
total	37.800	800	28.000	600			

TABLE I. Expected number of electron events in the unitary case coming from each relevant neutrino type. The detector is sensitive only to the total number of events, but the probability factor in the presence of non-unitarity is different for each incoming (anti)flavour. The error σ is taken as $\sigma^2 = \sigma_{\text{stat}}^2 + \sigma_{\text{sys}}^2$, where the statistical uncertainty $\sigma_{\text{stat}} = \sqrt{N}$ and the systematic uncertainty is taken as 2%, see text for details.

B. Neutrino-induced muon production

In order to be kinematically allowed, muon production requires more energetic neutrinos, with the kinematic threshold given by $E_\nu > (m_\mu^2 - m_e^2)/2m_e \approx 10$ GeV. While the flux peaks at a lower energy ~ 3 GeV, the tails can still generate a significant number of muon events in the final state, thus improving the sensitivity to the non-unitarity parameters. The number of events is given by

$$N_a^\mu = \mathcal{P}_a \mathcal{E} \int_{E_\nu^{\min}}^{\infty} \sigma(E_\nu) \lambda_a(E_\nu) dE_\nu, \quad (24)$$

where, again, \mathcal{E} is the exposure and $\lambda_a(E_\nu)$ is the flux.

\mathcal{N}_U $\nu_a + e^- \rightarrow \nu_j + \mu^-$	ν mode events	σ	$\bar{\nu}$ mode events	σ	$\mathcal{N}_{NU}/\mathcal{N}_U$ $\mathcal{P} G_F^2/G_\mu^2$	Seesaw order	Main contribution
ν_e	0	0	0	0	$ \alpha_{21} ^2$	$\mathcal{O}(\varepsilon^4)$	$\mathcal{O}(\varepsilon^4)$
ν_μ	17.900	400	14.200	300	α_{22}^2	$1 - \mathcal{O}(\varepsilon^2)$	CC
$\bar{\nu}_e$	380	20	230	20	α_{11}^2	$1 - \mathcal{O}(\varepsilon^2)$	CC
$\bar{\nu}_\mu$	0	0	0	0	$ \alpha_{21} ^2$	$\mathcal{O}(\varepsilon^4)$	$\mathcal{O}(\varepsilon^4)$
total	18.300	400	14.400	300			

TABLE II. Expected number of muon events in the unitary case coming from each species. The detector is sensitive only to the total event number, but the probability factor in the presence of non-unitarity differs for each incoming (anti)flavour. σ is $\sigma^2 = \sigma_{\text{stat}}^2 + \sigma_{\text{syst}}^2$, where $\sigma_{\text{stat}} = \sqrt{N}$ and the systematic uncertainty is taken as 2%, see text for details.

Note that now a denotes either the incoming muon neutrino or electron antineutrino. Muon antineutrino and electron neutrino flavours do not contribute to this process in the standard unitary case while, in the presence of non-unitarity, their contribution appears only as order $\mathcal{O}(\varepsilon^4)$ corrections. The results are given in Tab. II.

C. Analysis

We now proceed to estimate the sensitivity of our proposed leptonic-probe experiment to the non-unitarity parameters. In order to do so we take the χ^2 function as

$$\chi^2 = \sum_i \frac{(N_i^{\text{the}} - N_i^{\text{exp}})^2}{\sigma_{i, \text{stat}}^2 + \sigma_{i, \text{syst}}^2}, \quad (25)$$

where the subscript i runs over the 4 possible measurements: electron or muon events during the neutrino or antineutrino modes. Here N_i^{exp} is the number of detected events, while N_i^{the} is the expected number of events given as a function of the non-unitarity parameters and $\sigma_{i, \text{stat}}^2 = N_i^{\text{exp}}$.

In the analysis we will take different possible values for the systematic error, ranging from 0 – 3%, in order to account for the uncertainty in the flux calculation. We are aware that our benchmark assumption is too optimistic for the current setup, but it should serve as motivation for improvement, given the interest of the associated physics.

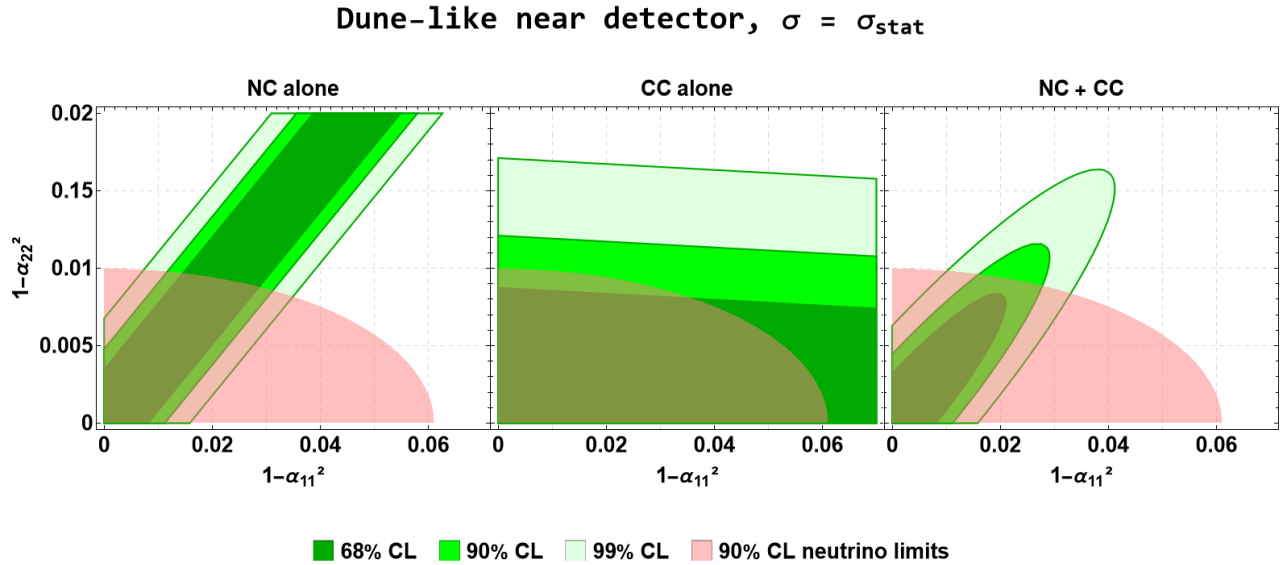


FIG. 3. The neutral current-dominated elastic neutrino-electron scattering process constrains the quantity $2\alpha_{22}^2 - \alpha_{11}^2$, while the purely charged current process $\nu_\mu + e^- \rightarrow \nu_j + \mu^-$ involves only α_{22}^2 . The combination of NC and CC events in the lepton channel constrains both non-unitarity parameters α_{11}^2 and α_{22}^2 . Here, for representation purposes, we show the sensitivity of a hypothetical experiment where the statistic uncertainty dominates the systematics. For comparison, the pink region represents the constraints from both long and short baseline experiments, as detailed in [48].

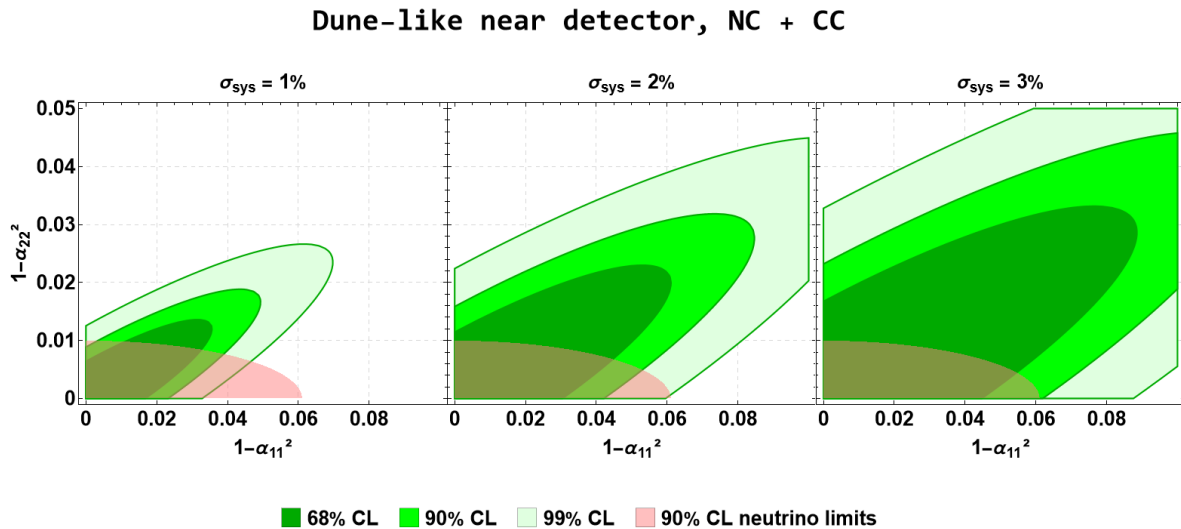


FIG. 4. Combination of the NC and CC results for different values of the systematic uncertainty. Again, the pink region represents the constraints from both long and short baseline experiments [48]. While the constraints on α_{22}^2 are already strong, this setup has the potential to significantly improve also the one on α_{11}^2 .

Notice that non-unitarity accounts for the fact that the heavy mediator states are not kinematically accessible. The direct effects of non-unitarity tend to decrease the event number, and this goes in the opposite direction

as the redefinition of the Fermi constant G_F discussed above. As a result, there is an intrinsic ambiguity in the electron events alone, leading to a parameter degeneracy. Note however that this ambiguity is not present in the charged current events, which are only sensitive to α_{22}^2 . Hence one can obtain a limit for both α_{11}^2 and α_{22}^2 only combining CC and NC event types. This behaviour can be seen in Fig. 3 where, for illustration purposes, an optimistic $\sigma = \sigma_{\text{stat}}$ uncertainty was assumed. We compare the recently updated “neutrino limits” extracted from neutrino oscillations at both long and short baseline experiments [48–51].

Our goal here is to focus more on the novelty of the measurement, rather than on the strength of the resulting sensitivities, as the setup is currently not optimized to do so. However, we can see that the attainable results can already be comparable to other similar experiments. In particular, the α_{11}^2 can be probed significantly better than current oscillation experiments [48]. It is worth noting that in general there are constraints arising from universality tests [52], electroweak precision measurements [47], such as the invisible Z decay [53], and charged Lepton Flavor Violation searches [54, 55]. For a recent extensive discussion see [56]. While the combination of these restrictions can be rather stringent, we stress the cleanliness of our proposed leptonic probe, and the fact that the interpretation is fairly model-independent.

In Fig. 4 we now consider the role of different values of the systematic uncertainty and again compare the resulting sensitivities with the current oscillation constraint.

Finally, we note that by combining the results from a DUNE-like near-detector with the oscillation constraints for different values of the systematic uncertainty, the measurement for α_{11}^2 can indeed improve, see Fig. 5. The fact that this happens even when the setup is not optimized for this type of measurement should serve as a motivation for the design of future experiments using leptonic neutral current as a way to underpin the neutrino mass generation seesaw mechanism.

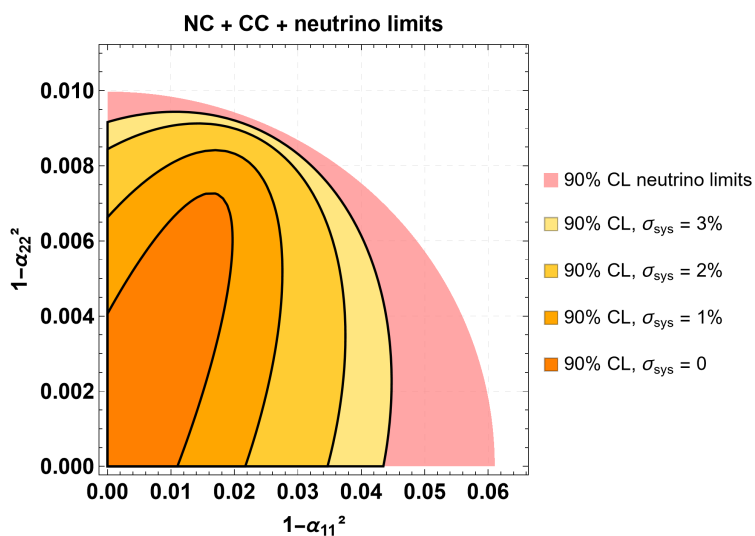


FIG. 5. Combination of the DUNE-like near detector measurement and the long and short baseline oscillation experiments constraints of [48] 90% CL for different values of the systematic uncertainty.

V. CONCLUSIONS AND OUTLOOK

Here we have proposed the use of leptonic probes, such as neutrino-electron scattering, as a viable way to test the non-minimal form of the charged and neutral leptonic weak interactions within a DUNE-like near-detector setup. Although the statistics is low, these processes are very clean and can provide complementary information to that available from oscillation studies. While the current setup is not optimized to our proposal, our results already indicate the potential for significant improvement on the sensitivities for the non-unitarity parameter α_{11}^2 when compared with current oscillation experiments. For example, Figs. 3, 4 and 5 illustrate how our method can help improving non-unitarity constraints and thereby shed light on the scale of neutrino mass generation within low-scale seesaw schemes. Last, but not least, our results further highlight the fact that a robust experimental setup for neutrino research requires the presence of near detectors. Moreover, these short-distance studies can provide, by themselves, valuable information on new physics parameters, such as the nonunitary parameters, an interesting physics goal by itself. Besides a plethora of low-energy probes [36–42], there are plenty of physics opportunities for testing unitarity violation. For example, through the searches for charged lepton flavor violating processes at low and high-energies [57–60]. One may also have the possibility of directly producing the TeV-scale neutrino-mass-mediators at colliders [61–72]. The rich variety of associated signals justifies the intense experimental effort devoted in present and upcoming experiments [73–79].

ACKNOWLEDGMENTS

We thank Joachim Kopp and Jaehoon Yu for insightful discussions. This work was supported by the Spanish grants PID2020-113775GB-I00 (AEI/10.13039/501100011033) and Prometeo CIPROM/2021/054 (Generalitat Valenciana). OGM was supported by the CONAHCyT grant 23238 and by SNII-México.

Appendix A: General formalism for neutrino and antineutrino scattering

Here we consider the general family of neutrino scattering processes $\nu_\alpha + e^- \rightarrow \nu + \ell_\beta^-$ and $\bar{\nu}_\alpha + e^- \rightarrow \bar{\nu} + \ell_\beta^-$ where α denotes the initial (anti)neutrino flavour, and the final lepton ℓ_β^- can be an electron, a muon or a tau, if kinematically possible. In other words, the initial (anti)neutrino is produced in association with a charged lepton of definite flavour. Moreover the neutrinos mix with new heavy mediator states. Since the final (anti)neutrino state is not measured, we sum over the three kinematically accessible neutral mass states j . We discuss the effect of non-unitarity at zero distance.

At tree level there is always a non-zero contribution coming from the charged current irrespective of α and β . However, we show that the cases in which this contribution vanishes in the unitary case are actually of order $\mathcal{O}(\varepsilon^4)$ in the presence of non-unitarity. On the other hand, when the probability factor is 1 in the standard case one now has a modification by a common factor of order $1 - \mathcal{O}(\varepsilon^2)$. For the NC there is only a non-zero contribution if $\beta = e$, in which case it is always of order $1 - \mathcal{O}(\varepsilon^2)$.

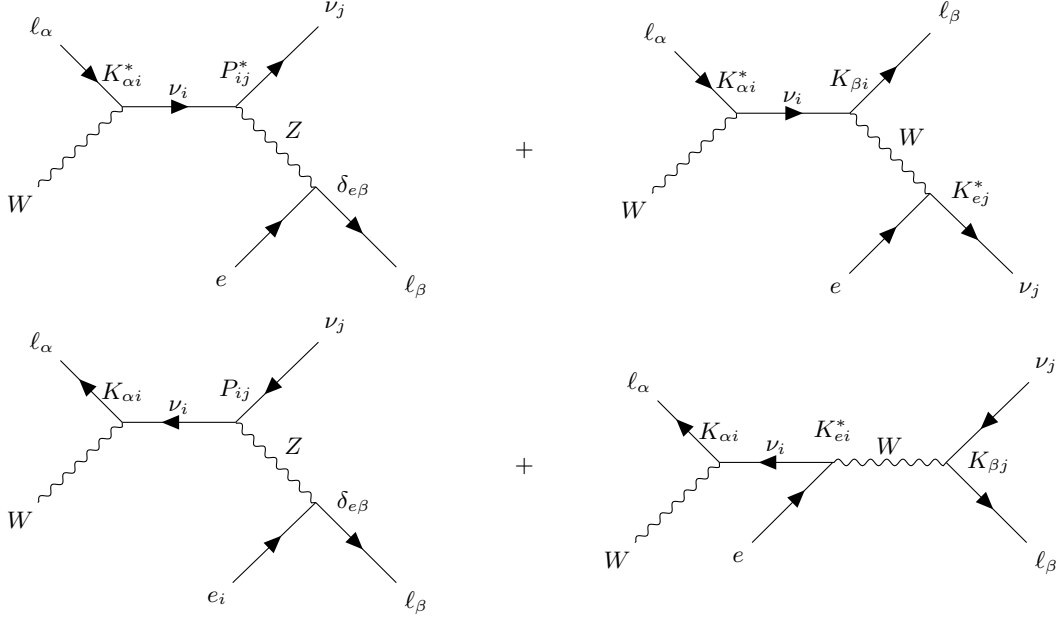


FIG. 6. Interplay between charged and neutral currents in the processes $\nu_\alpha + e^- \rightarrow \nu + \ell_\beta^-$ (upper row) and $\bar{\nu}_\alpha + e^- \rightarrow \bar{\nu} + \ell_\beta^-$ (lower row). The standard probability factors for each diagram are either 1 or 0, depending on the initial flavour α and the final charged lepton ℓ_β . However, in the presence of non-unitarity both diagrams are present, each carrying a different probability factor. Within a consistent seesaw expansion we show that the SM kinematic structure is preserved at order $\mathcal{O}(\varepsilon^2)$, see text for details.

1. Neutrino scattering

The full structure of the relevant diagrams is shown in the upper row of Fig. 6, while the relevant probability (and interference) factors are given in Eqs. A1-A3. Note that the probability factors are different for each combination of diagrams, i.e.

$$\mathcal{P}_{\alpha\beta}^{\text{NC}} = \delta_{e\beta} (NN^\dagger NN^\dagger NN^\dagger)_{\alpha\alpha} \quad (\text{A1})$$

$$\mathcal{P}_{\alpha\beta}^{\text{CC}} = (NN^\dagger)_{\alpha\beta} (NN^\dagger)_{\beta\alpha} (NN^\dagger)_{ee} \quad (\text{A2})$$

$$\mathcal{P}_{\alpha\beta}^{\text{int}} = \delta_{e\beta} (NN^\dagger)_{\beta\alpha} (NN^\dagger NN^\dagger)_{\alpha e} \quad (\text{A3})$$

Notice that α and β denote the fixed flavor indices associated to the survival or conversion probability, while the latin indices i, j are summed over, that is

$$(NN^\dagger)_{\alpha\beta} = \sum_{j=1}^3 N_{\alpha j} N_{j\beta}^\dagger.$$

Each of the probability factors in Eqs. A1-A3 affects different terms in the cross section, making the complete expression a complicated one. However, as already discussed for the particular ν_μ -electron elastic scattering case in Sec. III A, one finds that in general the kinematic structure of the SM is preserved at order $\mathcal{O}(\varepsilon^2)$.

Process	Contribution	\mathcal{P} factor at $\mathcal{O}(\varepsilon^2)$	$\mathcal{N}_{\text{NU}}/\mathcal{N}_{\text{U}} = \mathcal{P} G_F^2/G_\mu^2$	SM cross section	Kinematic threshold (Lab)
$\nu_e + e^- \rightarrow \nu_j + e^-$	NC+CC	$3\alpha_{11}^2 - 2$	$2\alpha_{11}^2 - \alpha_{22}^2$	Eq. A7	No
$\nu_\mu + e^- \rightarrow \nu_j + e^-$	NC	$3\alpha_{22}^2 - 2$	$2\alpha_{22}^2 - \alpha_{11}^2$	Eq. A8	
$\nu_\tau + e^- \rightarrow \nu_j + e^-$	NC	$3\alpha_{33}^2 - 2$	$3\alpha_{33}^2 - \alpha_{22}^2 - \alpha_{11}^2$	Eq. A8	
$\nu_e + e^- \rightarrow \nu_j + \mu^-$	CC	$\mathcal{O}(\varepsilon^4)$	$\mathcal{O}(\varepsilon^4)$	Eq. A9	$E_\nu > 10 \text{ GeV}$
$\nu_\mu + e^- \rightarrow \nu_j + \mu^-$		$2\alpha_{22}^2 + \alpha_{11}^2 - 2$	α_{22}^2		
$\nu_\tau + e^- \rightarrow \nu_j + \mu^-$		$\mathcal{O}(\varepsilon^4)$	$\mathcal{O}(\varepsilon^4)$		
$\nu_e + e^- \rightarrow \nu_j + \tau^-$	CC	$\mathcal{O}(\varepsilon^4)$	$\mathcal{O}(\varepsilon^4)$	Eq. A10	$E_\nu > 3 \text{ TeV}$
$\nu_\mu + e^- \rightarrow \nu_j + \tau^-$		$\mathcal{O}(\varepsilon^4)$	$\mathcal{O}(\varepsilon^4)$		
$\nu_\tau + e^- \rightarrow \nu_j + \tau^-$		$2\alpha_{33}^2 + \alpha_{11}^2 - 2$	$2\alpha_{33}^2 - \alpha_{22}^2$		

TABLE III. Structure of the family of processes $\nu_\alpha + e^- \rightarrow \nu + \ell_\beta^-$ in the presence of non-unitarity, including the probability factors at order $\mathcal{O}(\varepsilon^2)$, the kinematic factors for each contribution: NC, CC or the interference.

Modifications to the SM spectrum shape only come at order $\mathcal{O}(\varepsilon^4)$. For example, up to $\mathcal{O}(\varepsilon^2)$, one finds

$$\mathcal{P}_{\alpha\beta}^{\text{NC}} \approx \delta_{e\beta}(3\alpha_{\alpha\alpha}^2 - 2) + \mathcal{O}(\varepsilon^4) \sim \delta_{e\beta} \times [1 - \mathcal{O}(\varepsilon^2)] \quad (\text{A4})$$

$$\mathcal{P}_{\alpha\beta}^{\text{CC}} \approx \delta_{\alpha\beta}(2\alpha_{\alpha\alpha}^2 + \alpha_{11}^2 - 2) + \mathcal{O}(\varepsilon^4) \sim \delta_{\alpha\beta} \times [1 - \mathcal{O}(\varepsilon^2)] \quad (\text{A5})$$

$$\mathcal{P}_{\alpha\beta}^{\text{int}} \approx \delta_{e\beta}\delta_{\alpha\beta}(3\alpha_{11}^2 - 2) + \mathcal{O}(\varepsilon^4) \sim \delta_{e\beta}\delta_{\alpha\beta} \times [1 - \mathcal{O}(\varepsilon^2)] \quad (\text{A6})$$

From these one can easily conclude:

- In inelastic scattering processes (muon or tau neutrino-induced production), where the final charged lepton is not an electron, only the CC contribution exists. This corresponds to the case $\beta \neq e$.
- In elastic neutrino-electron scattering, $\beta = e$, if the initial neutrino flavour is of μ or τ type, $\alpha \neq e$, there is a CC contribution of order $\mathcal{O}(\varepsilon^4)$, subleading in comparison to the neutral current.
- If $\beta = e$ and the initial neutrino flavour is of electron type, $\alpha = e$, then the probability factors of the NC, the CC and the interference are all equal to $3\alpha_{11}^2 - 2$. This means that, again, there is no spectral distortion at order $\mathcal{O}(\varepsilon^2)$.

We emphasize that at tree-level and $\mathcal{O}(\varepsilon^2)$ in the seesaw expansion parameter the effect of non-unitarity is just a global factor times the SM prediction. This conclusion no longer holds at second order in the seesaw expansion, when the flavour-violating parameters of Eq. 3 come into play. In this case the $\mathcal{N}_{\text{NU}}/\mathcal{N}_{\text{U}}$ event number ratio will not be a constant and will instead depend on the kinematic parameters and flux shape.

A summary of these results is given in Tab. III, and the SM cross sections are given by

$$\frac{d\sigma}{dT}^{\text{NC+CC}}(\nu + e^- \rightarrow \nu + e^-) = \frac{2G_F^2 m_e}{\pi} \left((1 + g_L)^2 + g_R^2 \left(1 - \frac{T}{E\nu} \right)^2 - (1 + g_L)g_R \frac{m_e T}{E\nu^2} \right) \quad (\text{A7})$$

$$\frac{d\sigma}{dT}^{\text{NC}}(\nu + e^- \rightarrow \nu + e^-) = \frac{2G_F^2 m_e}{\pi} \left(g_L^2 + g_R^2 \left(1 - \frac{T}{E\nu} \right)^2 - g_L g_R \frac{m_e T}{E\nu^2} \right) \quad (\text{A8})$$

$$\sigma(\nu + e^- \rightarrow \nu + \mu^-) = \frac{G_F^2}{\pi} (2E\nu m_e - m_\mu^2) \quad (\text{A9})$$

Process	Contribution	\mathcal{P} factor at $\mathcal{O}(\varepsilon^2)$	$\mathcal{N}_{\text{NU}}/\mathcal{N}_{\text{U}} = \mathcal{P} G_F^2/G_\mu^2$	SM cross section	Kinematic threshold (Lab)
$\bar{\nu}_e + e^- \rightarrow \bar{\nu}_j + e^-$	NC+CC	$3\alpha_{11}^2 - 2$	$2\alpha_{11}^2 - \alpha_{22}^2$	Eq. A7, $(1 + g_L) \leftrightarrow g_R$	No
$\bar{\nu}_\mu + e^- \rightarrow \bar{\nu}_j + e^-$	NC	$3\alpha_{22}^2 - 2$	$2\alpha_{22}^2 - \alpha_{11}^2$	Eq. A8, $g_L \leftrightarrow g_R$	
$\bar{\nu}_\tau + e^- \rightarrow \bar{\nu}_j + e^-$	NC	$3\alpha_{33}^2 - 2$	$3\alpha_{33}^2 - \alpha_{22}^2 - \alpha_{11}^2$	Eq. A8, $g_L \leftrightarrow g_R$	
$\bar{\nu}_e + e^- \rightarrow \bar{\nu}_j + \mu^-$	CC	$2\alpha_{11}^2 + \alpha_{22}^2 - 2$	α_{11}^2	Eq. A9	$E_\nu > 10 \text{ GeV}$
$\bar{\nu}_\mu + e^- \rightarrow \bar{\nu}_j + \mu^-$		$\mathcal{O}(\varepsilon^4)$	$\mathcal{O}(\varepsilon^4)$		
$\bar{\nu}_\tau + e^- \rightarrow \bar{\nu}_j + \mu^-$		$\mathcal{O}(\varepsilon^4)$	$\mathcal{O}(\varepsilon^4)$		
$\bar{\nu}_e + e^- \rightarrow \bar{\nu}_j + \tau^-$	CC	$2\alpha_{11}^2 + \alpha_{33}^2 - 2$	$\alpha_{11}^2 - \alpha_{22}^2 + \alpha_{33}^2$	Eq. A10	$E_\nu > 3 \text{ TeV}$
$\bar{\nu}_\mu + e^- \rightarrow \bar{\nu}_j + \tau^-$		$\mathcal{O}(\varepsilon^4)$	$\mathcal{O}(\varepsilon^4)$		
$\bar{\nu}_\tau + e^- \rightarrow \bar{\nu}_j + \tau^-$		$\mathcal{O}(\varepsilon^4)$	$\mathcal{O}(\varepsilon^4)$		

TABLE IV. Summary of the family of processes $\bar{\nu}_\alpha + e^- \rightarrow \bar{\nu} + \ell_\beta^-$ in the presence of non-unitarity, including the probability factors at order $\mathcal{O}(\varepsilon^2)$, the kinematic factors and the contribution type: NC, CC or the interference.

$$\sigma(\nu + e^- \rightarrow \nu + \tau^-) = \frac{G_F^2}{\pi} (2E_\nu m_e - m_\tau^2) \quad (\text{A10})$$

2. Antineutrino scattering

While the results will be very similar to the neutrino case, we include them here for completeness. The diagrams are slightly different and are given by the lower row of Fig. 6, while their respective probability factors (and the interference) are given in Eqs. A11-A13.

$$\mathcal{P}_{\alpha\beta}^{\text{NC}} = \delta_{e\beta} (NN^\dagger NN^\dagger NN^\dagger)_{\alpha\alpha} \quad (\text{A11})$$

$$\mathcal{P}_{\alpha\beta}^{\text{CC}} = (NN^\dagger)_{\alpha e} (NN^\dagger)_{e\alpha} (NN^\dagger)_{\beta\beta} \quad (\text{A12})$$

$$\mathcal{P}_{\alpha\beta}^{\text{int}} = \delta_{e\beta} (NN^\dagger)_{e\alpha} (NN^\dagger NN^\dagger)_{\alpha\beta} \quad (\text{A13})$$

i.e. just replacing $e \leftrightarrow \beta$ in the neutrino case. Similar conclusions apply and a summary can be found in Tab. IV

-
- [1] T. Kajita, ‘‘Nobel Lecture: Discovery of atmospheric neutrino oscillations,’’ *Rev.Mod.Phys.* **88** (2016) 030501.
 - [2] A. B. McDonald, ‘‘Nobel Lecture: The Sudbury Neutrino Observatory: Observation of flavor change for solar neutrinos,’’ *Rev.Mod.Phys.* **88** (2016) 030502.
 - [3] **COHERENT** Collaboration, D. Akimov *et al.*, ‘‘Observation of Coherent Elastic Neutrino-Nucleus Scattering,’’ *Science* **357** no. 6356, (2017) 1123–1126, [arXiv:1708.01294 \[nucl-ex\]](#).
 - [4] **COHERENT** Collaboration, D. Akimov *et al.*, ‘‘COHERENT Collaboration data release from the first observation of coherent elastic neutrino-nucleus scattering,’’ [arXiv:1804.09459 \[nucl-ex\]](#).
 - [5] D. Z. Freedman, ‘‘Coherent Neutrino Nucleus Scattering as a Probe of the Weak Neutral Current,’’ *Phys. Rev. D* **9** (1974) 1389–1392.
 - [6] A. Drukier and L. Stodolsky, ‘‘Principles and Applications of a Neutral Current Detector for Neutrino Physics and Astronomy,’’ *Phys. Rev. D* **30** (1984) 2295.

- [7] J. Schechter and J. W. F. Valle, “Neutrino Masses in SU(2) x U(1) Theories,” *Phys.Rev.D* **22** (1980) 2227.
- [8] J. Schechter and J. W. F. Valle, “Neutrino Decay and Spontaneous Violation of Lepton Number,” *Phys.Rev.D* **25** (1982) 774.
- [9] J. W. F. Valle, “Resonant Oscillations of Massless Neutrinos in Matter,” *Phys.Lett.* **B199** (1987) 432–436.
- [10] H. Nunokawa *et al.*, “Resonant conversion of massless neutrinos in supernovae,” *Phys.Rev.* **D54** (1996) 4356–4363.
- [11] D. Grasso, H. Nunokawa, and J. W. F. Valle, “Pulsar velocities without neutrino mass,” *Phys.Rev.Lett.* **81** (1998) 2412–2415.
- [12] R. Mohapatra and J. W. F. Valle, “Neutrino Mass and Baryon Number Nonconservation in Superstring Models,” vol. 34, p. 1642. 1986.
- [13] M. Gonzalez-Garcia and J. W. F. Valle, “Fast Decaying Neutrinos and Observable Flavor Violation in a New Class of Majoron Models,” *Phys.Lett.* **B216** (1989) 360–366.
- [14] E. K. Akhmedov *et al.*, “Left-right symmetry breaking in NJL approach,” *Phys.Lett.B* **368** (1996) 270–280, [arXiv:hep-ph/9507275 \[hep-ph\]](#).
- [15] E. K. Akhmedov *et al.*, “Dynamical left-right symmetry breaking,” *Phys.Rev.D* **53** (1996) 2752–2780, [arXiv:hep-ph/9509255 \[hep-ph\]](#).
- [16] M. Malinsky, J. Romao, and J. W. F. Valle, “Novel supersymmetric SO(10) seesaw mechanism,” *Phys.Rev.Lett.* **95** (2005) 161801, [arXiv:hep-ph/0506296 \[hep-ph\]](#).
- [17] F. Escrivehuela *et al.*, “On the description of nonunitary neutrino mixing,” *Phys.Rev.* **D92** (2015) 053009, [arXiv:1503.08879 \[hep-ph\]](#).
- [18] F. Escrivehuela, D. Forero, O. Miranda, M. Tórtola, and J. W. F. Valle, “Probing CP violation with non-unitary mixing in long-baseline neutrino oscillation experiments: DUNE as a case study,” *New J.Phys.* **19** (2017) 093005, [arXiv:1612.07377 \[hep-ph\]](#).
- [19] C. S. Fong, H. Minakata, and H. Nunokawa, “A framework for testing leptonic unitarity by neutrino oscillation experiments,” *JHEP* **02** (2017) 114, [arXiv:1609.08623 \[hep-ph\]](#).
- [20] S.-F. Ge, P. Pasquini, M. Tortola, and J. W. F. Valle, “Measuring the leptonic CP phase in neutrino oscillations with nonunitary mixing,” *Phys.Rev.* **D95** (2017) 033005, [arXiv:1605.01670 \[hep-ph\]](#).
- [21] O. Miranda and J. W. F. Valle, “Neutrino oscillations and the seesaw origin of neutrino mass,” *Nucl.Phys.* **B908** (2016) 436–455, [arXiv:1602.00864 \[hep-ph\]](#).
- [22] O. Miranda, M. Tortola, and J. W. F. Valle, “New ambiguity in probing CP violation in neutrino oscillations,” *Phys.Rev.Lett.* **117** (2016) 061804, [arXiv:1604.05690 \[hep-ph\]](#).
- [23] C. S. Fong, H. Minakata, and H. Nunokawa, “Non-unitary evolution of neutrinos in matter and the leptonic unitarity test,” *JHEP* **02** (2019) 015, [arXiv:1712.02798 \[hep-ph\]](#).
- [24] L. S. Miranda, P. Pasquini, U. Rahaman, and S. Razzaque, “Searching for non-unitary neutrino oscillations in the present T2K and NO ν A data,” *Eur. Phys. J. C* **81** no. 5, (2021) 444, [arXiv:1911.09398 \[hep-ph\]](#).
- [25] O. G. Miranda, D. K. Papoulias, O. Sanders, M. Tórtola, and J. W. F. Valle, “Future CE ν NS experiments as probes of lepton unitarity and light-sterile neutrinos,” *Phys. Rev. D* **102** (2020) 113014, [arXiv:2008.02759 \[hep-ph\]](#).
- [26] I. Martinez-Soler and H. Minakata, “Measuring tau neutrino appearance probability via unitarity,” *Phys. Rev. D* **104** no. 9, (2021) 093006, [arXiv:2109.06933 \[hep-ph\]](#).
- [27] U. Rahaman and S. Razzaque, “Non-Unitary Neutrino Mixing in the NO ν A Near Detector Data,” *Universe* **8** no. 4, (2022) 238, [arXiv:2108.11783 \[hep-ph\]](#).
- [28] C. Soumya, “Probing nonunitary neutrino mixing via long-baseline neutrino oscillation experiments based at J-PARC,” *Phys. Rev. D* **105** no. 1, (2022) 015012, [arXiv:2104.04315 \[hep-ph\]](#).

- [29] D. Kaur, N. R. K. Chowdhury, and U. Rahaman, “Effect of non-unitary mixing on the mass hierarchy and CP violation determination at the Protvino to Orca experiment,” [arXiv:2110.02917 \[hep-ph\]](#).
- [30] Y. Wang and S. Zhou, “Non-unitary leptonic flavor mixing and CP violation in neutrino-antineutrino oscillations,” *Phys. Lett. B* **824** (2022) 136797, [arXiv:2109.13622 \[hep-ph\]](#).
- [31] S. S. Chatterjee, O. G. Miranda, M. Tórtola, and J. W. F. Valle, “Nonunitarity of the lepton mixing matrix at the European Spallation Source,” *Phys. Rev. D* **106** no. 7, (2022) 075016, [arXiv:2111.08673 \[hep-ph\]](#).
- [32] S. Gariazzo, P. Martínez-Miravé, O. Mena, S. Pastor, and M. Tórtola, “Non-unitary three-neutrino mixing in the early Universe,” *JCAP* **03** (2023) 046, [arXiv:2211.10522 \[hep-ph\]](#).
- [33] D. Aloni and A. Dery, “Revisiting leptonic non-unitarity in light of FASER ν ,” [arXiv:2211.09638 \[hep-ph\]](#).
- [34] S. Sahoo, S. Das, A. Kumar, and S. K. Agarwalla, “Constraining non-unitary neutrino mixing using matter effects in atmospheric neutrinos at INO-ICAL,” [arXiv:2309.16942 \[hep-ph\]](#).
- [35] J. M. Celestino-Ramírez, F. J. Escrihuela, L. J. Flores, and O. G. Miranda, “Testing the non-unitarity of the leptonic mixing matrix at FASER,” [arXiv:2309.00116 \[hep-ph\]](#).
- [36] O. G. Miranda, D. K. Papoulias, O. Sanders, M. Tórtola, and J. W. F. Valle, “Low-energy probes of sterile neutrino transition magnetic moments,” *JHEP* **12** (2021) 191, [arXiv:2109.09545 \[hep-ph\]](#).
- [37] T. Schwetz and A. Segarra, “T violation in nonstandard neutrino oscillation scenarios,” *Phys. Rev. D* **105** no. 5, (2022) 055001, [arXiv:2112.08801 \[hep-ph\]](#).
- [38] T. Schwetz and A. Segarra, “Model-Independent Test of T Violation in Neutrino Oscillations,” *Phys. Rev. Lett.* **128** no. 9, (2022) 091801, [arXiv:2106.16099 \[hep-ph\]](#).
- [39] J. Tang, S. Vihonen, and Y. Xu, “Precision measurements and tau neutrino physics in a future accelerator neutrino experiment,” *Commun. Theor. Phys.* **74** no. 3, (2022) 035201, [arXiv:2108.11107 \[hep-ph\]](#).
- [40] J. Arrington *et al.*, “Physics Opportunities for the Fermilab Booster Replacement,” [arXiv:2203.03925 \[hep-ph\]](#).
- [41] F. Capozzi, C. Giunti, and C. A. Ternes, “Improved sensitivities of ESS ν SB from a two-detector fit,” *JHEP* **04** (2023) 130, [arXiv:2302.07154 \[hep-ph\]](#).
- [42] S. R. Soleti, P. Coloma, J. J. G. Cadenas, and A. Cabrera, “Search for Hidden Neutrinos at the European Spallation Source: the SHiNESS experiment,” [arXiv:2311.18509 \[hep-ex\]](#).
- [43] O. Miranda *et al.*, “Exploring the Potential of Short-Baseline Physics at Fermilab,” *Phys.Rev.* **D97** (2018) 095026, [arXiv:1802.02133 \[hep-ph\]](#).
- [44] P. Coloma, J. López-Pavón, S. Rosauero-Alcaraz, and S. Urrea, “New physics from oscillations at the DUNE near detector, and the role of systematic uncertainties,” *JHEP* **08** (2021) 065, [arXiv:2105.11466 \[hep-ph\]](#).
- [45] P. de Salas *et al.*, “2020 global reassessment of the neutrino oscillation picture,” *JHEP* **02** (2021) 071, [arXiv:2006.11237 \[hep-ph\]](#).
- [46] M. Blennow, P. Coloma, E. Fernandez-Martinez, J. Hernandez-Garcia, and J. Lopez-Pavon, “Non-Unitarity, sterile neutrinos, and Non-Standard neutrino Interactions,” *JHEP* **04** (2017) 153, [arXiv:1609.08637 \[hep-ph\]](#).
- [47] **Particle Data Group** Collaboration, R. L. Workman and Others, “Review of Particle Physics,” *PTEP* **2022** (2022) 083C01.
- [48] D. Forero, C. Giunti, C. Ternes, and M. Tortola, “Non-unitary neutrino mixing in short and long-baseline experiments,” [arXiv:2103.01998 \[hep-ph\]](#).
- [49] Z. Hu, J. Ling, J. Tang, and T. Wang, “Global oscillation data analysis on the 3ν mixing without unitarity,” *JHEP* **01** (2021) 124, [arXiv:2008.09730 \[hep-ph\]](#).
- [50] S. A. R. Ellis, K. J. Kelly, and S. W. Li, “Current and Future Neutrino Oscillation Constraints on Leptonic Unitarity,” *JHEP* **12** (2020) 068, [arXiv:2008.01088 \[hep-ph\]](#).
- [51] S. K. Agarwalla, S. Das, A. Giarnetti, and D. Meloni, “Model-independent constraints on non-unitary neutrino mixing from high-precision long-baseline experiments,” *JHEP* **07** (2022) 121, [arXiv:2111.00329 \[hep-ph\]](#).

- [52] D. Bryman, V. Cirigliano, A. Crivellin, and G. Inguglia, “Testing Lepton Flavor Universality with Pion, Kaon, Tau, and Beta Decays,” *Ann.Rev.Nucl.Part.Sci.* **72** (2022) 69–91, [arXiv:2111.05338 \[hep-ph\]](#).
- [53] F. J. Escrihuela, L. J. Flores, and O. G. Miranda, “Neutrino counting experiments and non-unitarity from LEP and future experiments,” *Phys. Lett. B* **802** (2020) 135241, [arXiv:1907.12675 \[hep-ph\]](#).
- [54] D. Forero, S. Morisi, M. Tortola, and J. W. F. Valle, “Lepton flavor violation and non-unitary lepton mixing in low-scale type-I seesaw,” *JHEP* **09** (2011) 142, [arXiv:1107.6009 \[hep-ph\]](#).
- [55] M. Lindner, M. Platscher, and F. S. Queiroz, “A Call for New Physics : The Muon Anomalous Magnetic Moment and Lepton Flavor Violation,” *Phys. Rept.* **731** (2018) 1–82, [arXiv:1610.06587 \[hep-ph\]](#).
- [56] M. Blennow, E. Fernández-Martínez, J. Hernández-García, J. López-Pavón, X. Marcano, and D. Naredo-Tuero, “Bounds on lepton non-unitarity and heavy neutrino mixing,” *JHEP* **08** (2023) 030, [arXiv:2306.01040 \[hep-ph\]](#).
- [57] J. Bernabeu *et al.*, “Lepton Flavor Nonconservation at High-Energies in a Superstring Inspired Standard Model,” *Phys.Lett.B* **187** (1987) 303–308.
- [58] M. Gonzalez-Garcia and J. W. F. Valle, “Fast Decaying Neutrinos and Observable Flavor Violation in a New Class of Majoron Models,” *Phys.Lett.B* **216** (1989) 360–366.
- [59] A. Abada, M. E. Krauss, W. Porod, F. Staub, A. Vicente, and C. Weiland, “Lepton flavor violation in low-scale seesaw models: SUSY and non-SUSY contributions,” *JHEP* **11** (2014) 048, [arXiv:1408.0138 \[hep-ph\]](#).
- [60] C. Hagedorn, J. Kriewald, J. Orloff, and A. M. Teixeira, “Flavour and CP symmetries in the inverse seesaw,” *Eur. Phys. J. C* **82** no. 3, (2022) 194, [arXiv:2107.07537 \[hep-ph\]](#).
- [61] M. Dittmar, A. Santamaria, M. Gonzalez-Garcia, and J. W. F. Valle, “Production Mechanisms and Signatures of Isosinglet Neutral Heavy Leptons in Z^0 Decays,” *Nucl.Phys.B* **332** (1990) 1–19.
- [62] M. Gonzalez-Garcia, A. Santamaria, and J. W. F. Valle, “Isosinglet Neutral Heavy Lepton Production in Z Decays and Neutrino Mass,” *Nucl.Phys.B* **342** (1990) 108–126.
- [63] A. Atre, T. Han, S. Pascoli, and B. Zhang, “The Search for Heavy Majorana Neutrinos,” *JHEP* **05** (2009) 030, [arXiv:0901.3589 \[hep-ph\]](#).
- [64] J. Aguilar-Saavedra *et al.*, “Flavour in heavy neutrino searches at the LHC,” *Phys.Rev.D* **85** (2012) 091301, [arXiv:1203.5998 \[hep-ph\]](#).
- [65] S. Das, F. Deppisch, O. Kittel, and J. W. F. Valle, “Heavy Neutrinos and Lepton Flavour Violation in Left-Right Symmetric Models at the LHC,” *Phys.Rev.D* **86** (2012) 055006, [arXiv:1206.0256 \[hep-ph\]](#).
- [66] F. F. Deppisch, N. Desai, and J. W. F. Valle, “Is charged lepton flavor violation a high energy phenomenon?,” *Phys.Rev.D* **89** (2014) 051302, [arXiv:1308.6789 \[hep-ph\]](#).
- [67] S. Antusch and O. Fischer, “Testing sterile neutrino extensions of the Standard Model at future lepton colliders,” *JHEP* **05** (2015) 053, [arXiv:1502.05915 \[hep-ph\]](#).
- [68] F. F. Deppisch, P. S. Bhupal Dev, and A. Pilaftsis, “Neutrinos and Collider Physics,” *New J. Phys.* **17** no. 7, (2015) 075019, [arXiv:1502.06541 \[hep-ph\]](#).
- [69] M. Hirsch and Z. S. Wang, “Heavy neutral leptons at ANUBIS,” *Phys. Rev. D* **101** no. 5, (2020) 055034, [arXiv:2001.04750 \[hep-ph\]](#).
- [70] G. Cottin *et al.*, “Long-lived heavy neutral leptons with a displaced shower signature at CMS,” *JHEP* **02** (2023) 011, [arXiv:2210.17446 \[hep-ph\]](#).
- [71] G. Chauhan, P. S. B. Dev, I. Dubovyk, B. Dziewit, W. Flieger, K. Grzanka, J. Gluza, B. Karmakar, and S. Zieba, “Phenomenology of Lepton Masses and Mixing with Discrete Flavor Symmetries, ,” [arXiv:2310.20681 \[hep-ph\]](#).
- [72] A. Batra, P. Bharadwaj, S. Mandal, R. Srivastava, and J. W. F. Valle, “Phenomenology of the simplest linear seesaw mechanism,” *JHEP* **07** (2023) 221, [arXiv:2305.00994 \[hep-ph\]](#).
- [73] S. Alekhin *et al.*, “A facility to Search for Hidden Particles at the CERN SPS: the SHiP physics case,” *Rept. Prog. Phys.* **79** no. 12, (2016) 124201, [arXiv:1504.04855 \[hep-ph\]](#).

- [74] **CMS** Collaboration, “Search for heavy Majorana neutrinos in the same-sign dilepton channel in proton-proton collisions at $\sqrt{s} = 13$ TeV,”
- [75] **ATLAS** Collaboration, M. Aaboud *et al.*, “Search for heavy Majorana or Dirac neutrinos and right-handed W gauge bosons in final states with two charged leptons and two jets at $\sqrt{s} = 13$ TeV with the ATLAS detector,” *JHEP* **01** (2019) 016, [arXiv:1809.11105 \[hep-ex\]](#).
- [76] J. Alimena *et al.*, “Searching for long-lived particles beyond the Standard Model at the Large Hadron Collider,” *J. Phys. G* **47** no. 9, (2020) 090501, [arXiv:1903.04497 \[hep-ex\]](#).
- [77] **CMS** Collaboration, A. Tumasyan *et al.*, “Search for long-lived heavy neutral leptons with displaced vertices in proton-proton collisions at $\sqrt{s} = 13$ TeV,” *JHEP* **07** (2022) 081, [arXiv:2201.05578 \[hep-ex\]](#).
- [78] A. M. Abdullahi *et al.*, “The present and future status of heavy neutral leptons,” *J. Phys. G* **50** no. 2, (2023) 020501, [arXiv:2203.08039 \[hep-ph\]](#).
- [79] **CMS** Collaboration, “Search for long-lived heavy neutral leptons with lepton flavour conserving or violating decays to a jet and a charged lepton,” [arXiv:2312.07484 \[hep-ex\]](#).